Membrane-based TBADT recovery: increasing the sustainability of continuous-flow photocatalytic HAT transformations

Zhenghui Wen[1,+], Diego Pintossi[1,+], Manuel Nuño,[2] Timothy Noël[1]*

[1] Flow Chemistry Group, Van 't Hoff Institute for Molecular Sciences, Faculty of Science, University of Amsterdam, Science Park 904, 1098 XH Amsterdam, The Netherlands.

[2] Vapourtec Ltd., Park Farm Business Centre, Fornham St Genevieve, Bury St Edmunds, Suffolk IP28 6TS, United Kingdom.

[+] These authors equally contributed to the manuscript.

*Corresponding author: t.noel@uva.nl

Keywords: flow chemistry, hydrogen atom transfer, catalyst recovery, organic solvent nanofiltration, decatungstate, C−H functionalization, photocatalysis, homogeneous catalysis

Abstract

Photocatalytic hydrogen atom transfer (HAT) processes have been the object of numerous studies showcasing the potential of the homogeneous photocatalyst tetrabutylammonium decatungstate (TBADT) for the functionalization of C(sp^3)–H bonds. However, to translate these studies into large-scale industrial processes, careful considerations of catalyst consumption, cost, and removal are required. This work presents organic solvent nanofiltration (OSN) as the answer to reduce TBADT consumption, to increase its turnover number and to lower its concentration in the product solution, thus enabling large-scale photocatalytic HAT-based transformations. The operating parameters for a suitable membrane for TBADT recovery in acetonitrile were optimized. Continuous photocatalytic C(sp^3)-H alkylation reactions were carried out with in-line TBADT recovery via two OSN steps. Promisingly, the observed product yields for the reactions with in-line catalyst recycling are comparable to those of reactions performed with pristine TBADT, therefore highlighting that not only catalyst recovery (>99%, TON > 6500) is a possibility, but also that it does not happen at the expense of reaction performance.

Introduction

In recent years, light-induced hydrogen atom transfer (HAT) presented itself as a versatile strategy for the late-stage functionalization of C(sp^3)–H bonds without involving transition-metal catalysis or strong oxidants.[1, 2] In HAT, the photoexcited catalyst abstracts a hydrogen atom resulting in the formation of reactive radical species, which are exploited for highly selective functionalization. To achieve this selectivity, careful tuning of the steric and electric properties of the HAT photocatalyst and substrate has to take place. Among the limited selection of photocatalysts promoting HAT, arguably the most versatile HAT photocatalyst is the decatungstate anion, which found application in a wide range of transformations, including alkylation,[3-8] arylation,[9] acylation,[10] amination[11-14], fluorination,[15-17] trifluoromethylation,[18] sulfinylation[19] and oxygenation (Scheme 1A).[20, 21]

Despite the potential of TBADT for synthetic applications, the adoption of photocatalytic HAT in industrial processes is still limited. To understand this, one has to consider that while catalyst cost and removal or recycling are minor concerns in demonstrating a new synthetic method, these aspects become major focal points in the transition from small scale (e.g., required in medicinal chemistry and academia) to large-scale production (Scheme 1B-C).[22,23] Therefore, among the main hurdles hindering its adoption, the primary concerns are the questions surrounding the ability to scale up photocatalytic HAT reactions paired with the need to recycle the catalyst[24] and the requirement to purify the product.[25] The former concern about scalability has been addressed in recent years when continuous-flow chemistry systems proved to be the answer to the scale-up needs of photochemical reactions, as was highlighted in several examples of large-scale photochemical reactions carried out in continuous-flow systems.[11, 26-31] For the removal of the catalyst, organic solvent nanofiltration (OSN) could be a suitable strategy for catalyst recovery in continuous-flow systems. OSN is a membrane-based process where selective separation of the species present in solution is obtained based on their size.[32-35] Molecules smaller than the so-called molecular weight cut-off (MWCO) of the membrane will pass through the membrane, while species larger than the MWCO are selectively retained. Typical MWCO values for

commercial OSN membranes range from 150 to 1000 Da, thus making them ideal for the selective separation between homogeneous catalysts having a large molecular weight, such as TBADT, and smaller reaction products.[34, 36] Additionally, OSN has the distinct advantage of low energy requirements since phase transitions such as evaporation are avoided in this separation technique. The absence of thermal transitions also removes the issue of thermal stress for the recovered catalyst, which is present in other recovery techniques. The work of Livingston and co-workers highlighted the performance of OSN with commercial membranes for the recovery of a homogeneous catalyst in Heck couplings performed in continuous flow.[37] Additionally, recent studies from Guerra et al. and O'Neal and Jensen demonstrated the suitability of coupling OSN for catalyst recovery with flow microreactors. Guerra et al. demonstrated the use of OSN to recover homogeneous catalyst complexes in a hydroformylation reaction.[36] Similarly, O'Neal and Jensen implemented a small-scale custom OSN unit in an automated setup performing ring-closing metathesis with a recycled second-generation Hoveyda-Grubbs catalyst.[38] Although recent works showcased the potential of OSN in flow chemistry, they also highlighted the challenges of catalyst deactivation and membrane fouling.

Herein, we describe a continuous-flow system coupling a micro-flow photoreactor with OSN-based in-line TBADT recovery (Scheme 1D). The performance of photocatalytic HAT in the form of various photocatalytic C(sp^3)–H alkylation reactions carried out with recycled TBADT (Scheme 2A) were investigated in conjunction with a two-stage OSN unit for the in-line recovery of TBADT (Scheme 2B), proving the concept of scalable TBADT-based HAT transformations with low catalyst consumption and high turnover number (TON).

A Photocatalytic Hydrogen Atom Transfer (HAT): a convenient strategy for C(sp^3)–H functionalization.

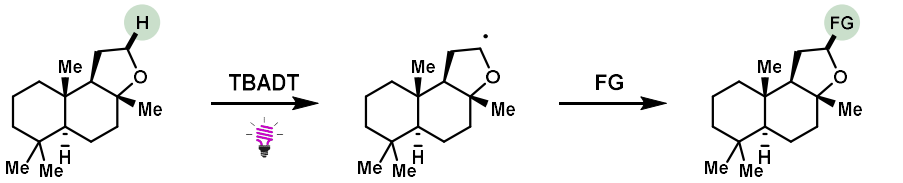

B Medicinal chemistry versus process chemistry: a challenging, time-constrained transition.

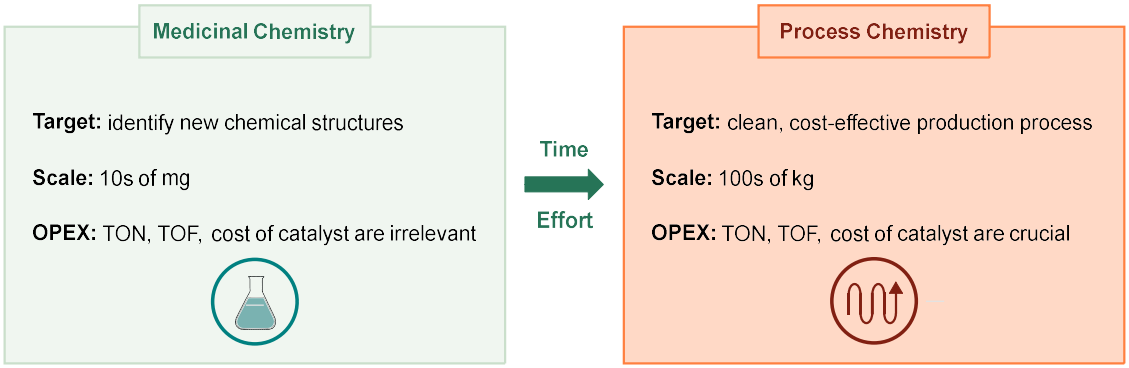

C Large molecular weight of decatungstate photocatalyst leads to high mass fraction in reaction mixture.

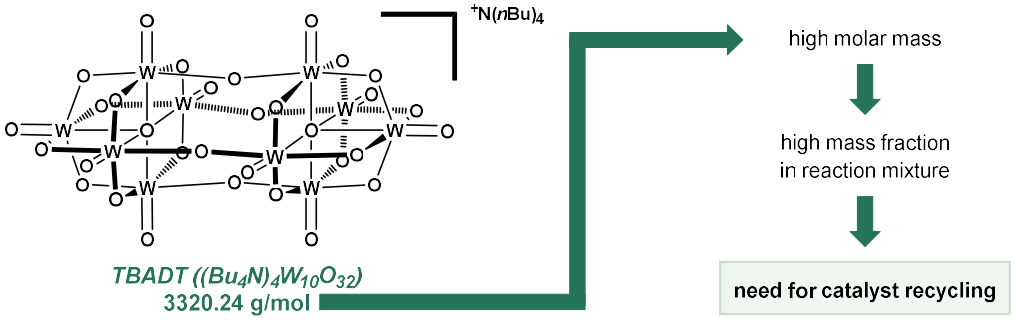

D This work: Inline nanofiltration enables high recovery and recycling of decatungstate in continuous flow.

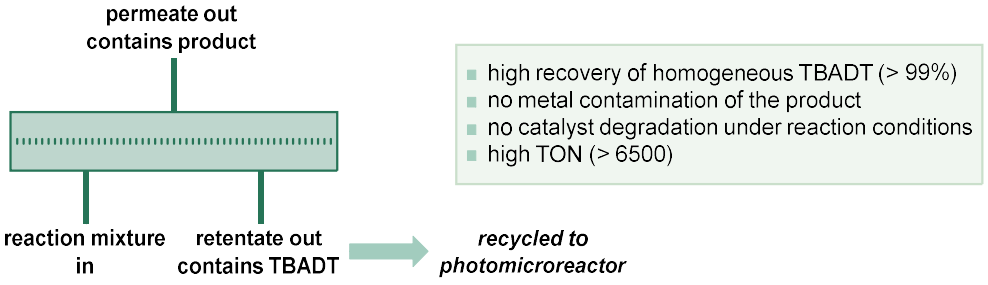

84
85

Scheme 1. (A) Photocatalytic Hydrogen Atom Transfer enables both early- and late-stage functionalization of hydroalkanes and biologically active compounds. (B) Small scale versus large scale synthetic organic chemistry require different approaches: catalyst lifetime and cost are only relevant on a process chemistry level. (C) TBADT is a high molecular weight molecule resulting in a large mass fraction and thus high associated cost when discarded. This warrants the need for catalyst recycling. (D) We disclose a general and efficient approach for decatungstate recycling using inline nanofiltration.

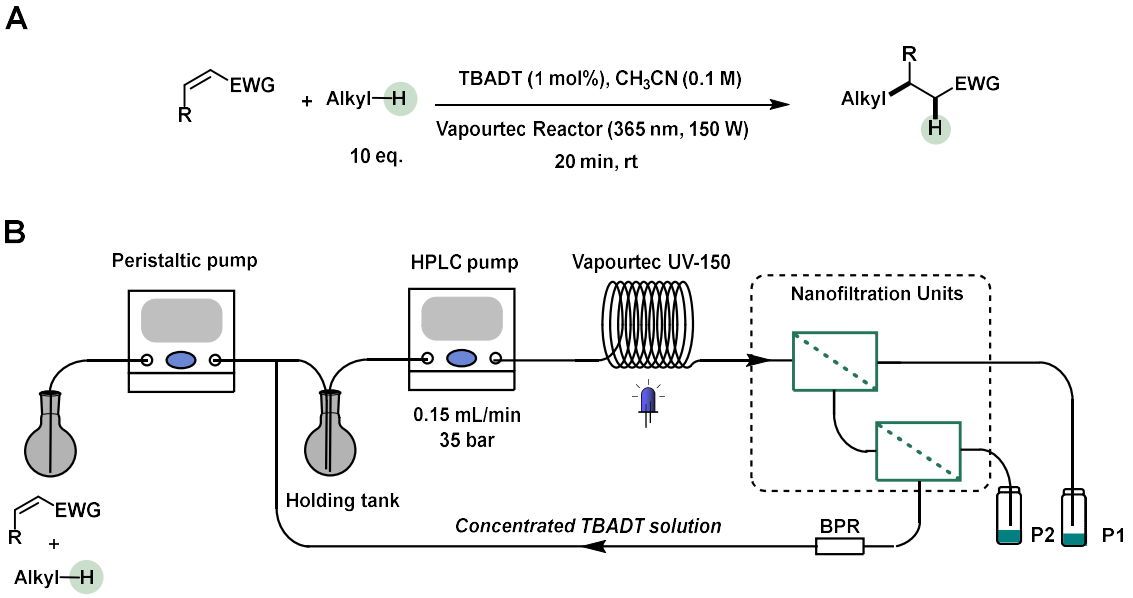

Scheme 2 (A) TBADT-catalyzed C(sp^3)–H alkylation investigated in the present work. (B) flow chart of the multi-stage nanofiltration-based continuous flow system employed for the recovery of TBADT.

Results and discussion

To achieve a successful C(sp^3)–H functionalization reaction in continuous flow with inline catalyst recycling via nanofiltration, suitable commercial membranes were initially evaluated. While the large molecular weight and stability of TBADT make it an ideal candidate for membrane-based recovery, its poor solubility in solvents other than acetonitrile

and acetone[20] represents a significant challenge due to the limited compatibility of commercial OSN membranes with such solvents. Commercial membranes were screened using a Zaiput 10 cross-flow cell and by measuring the flux and selectivity during filtration of 1 mM TBADT solutions in acetonitrile (see Supplementary Information, section 2.1, Figure S1-2). Of the membrane pool taken into consideration, only NF080105 and NF030306 from SolSep BV could withstand filtration experiments in acetonitrile. Therefore, these membranes were chosen for further testing involving longer experiment times and higher pressures, which highlighted the unsuitability of NF080105 due to a high failure rate during prolonged filtration experiments paired with issues of catalyst accumulation in the membrane, which negatively affected the membrane flux and mass balance during the filtration (Supplementary Information, Section 2.5, Figure S10). Therefore, the outcome of the membrane screening was that NF030306 is a suitable membrane for OSN of acetonitrile solutions containing TBADT. An important consideration is that the high chemical resistance of this membrane comes at the expense of a relatively low membrane flux, resulting in a limited permeate-to-retentate ratio. However, this issue can be obviated with an appropriate design of the filtration stages, as shown in the discussion below.

Once a membrane candidate was secured, the following step was optimizing filtration performance as a function of operating pressure and input flow rate. As the Zaiput cell was limited to 20 bar maximum pressure, a new cross-flow cell was designed in-house to achieve pressures up to 40 bar (operating limit for the NF030306, according to its specifications). The cell design is detailed in Supplementary Information, Section 2.6. Figure S1 in Supplementary Information presents the results of the screening of operating pressures of TBADT recovery with nanofiltration. As expected, higher pressures resulted in an increased flux without significantly affecting TBADT recovery. However, at 40 bar, undesired TBADT precipitation occurred, leading to decreased catalyst concentration in the retentate solution and, thus, reduced catalyst recovery. For this reason, an operating pressure of 35 bar was selected for further experiments. Figure S19 in Supplementary Information details the screening of flow rates. Longer residence times in the cell resulted in

increased transport across the membrane. However, a decreased flux was observed for the lowest flow rate, which can be explained by reduced mixing in the cell and concentration polarization across the membrane. Therefore, the flow rate for catalyst recovery was maintained at 0.15 mL/min. The result of the membrane screening and operating parameters optimization proved the potential of OSN for TBADT recovery, with an achieved recovery exceeding 98%.

The potential negative impact on catalyst activity of the recycling process was taken into consideration and tested by performing alkylation reactions with TBADT that was obtained either via OSN or via non-solvent extraction and filtration. In both cases, product yields comparable to those achieved with pristine TBADT were measured (Figure S20 and Table S2 in Supplementary Information). This result highlights that catalyst recycling has no observable detrimental effects on the stability and catalytic activity of TBADT. We believe this is due to the molecular structure of TBADT which is not prone for radical attack. This is in contrast to organic dyes and Ru- or Ir-based photocatalysts where the ligands, often polypyridyl moieties, are excellent acceptors for radicals and are the main cause for catalyst degradation.[39]

When moving from TBADT solution to the reaction mixture, undesired interactions of substances in the reaction mixture, such as starting materials, products or byproducts, with the membrane may negatively affect filtration performance. Therefore, to evaluate potentially undesired effects of chemicals present in the reaction mixture, filtration experiments were performed with mixtures containing an increasing number of substances: TBADT, TBADT and cyclohexane, and the complete reaction mixture. For all experiments, comparable fluxes were observed (Figure S21 in Supplementary Information). Therefore, a negative influence of reaction components, particularly cyclohexane, was ruled out.

The model reaction chosen to investigate in-line catalyst recovery was the same alkylation reaction optimized by Wen et al.,[4] albeit with a different substrate (dimethyl maleate). The starting material was changed to avoid any UV-vis absorbance of the substrate and product in the same wavelength range of the TBADT peak, thus enabling

160 determination of the TBADT concentration from the measurement of UV-vis spectra of the
161 retentate and permeate streams obtained during filtration experiments. The validity of the
162 previously identified optimal reaction conditions was confirmed by varying the catalyst
163 loading, the number of cyclohexane equivalents, and the residence time of the reaction
164 involving the new substrate (Tables S3–5 in Supplementary Information).
165 To design the inline continuous-flow catalyst recycling, detailed knowledge of the OSN
166 performance with the solution collected at the outlet of the flow reactor was key. Therefore, a
167 batch study was performed by collecting and filtering the solution resulting from the model
168 alkylation reaction (Figure 1a). Encouraging results were obtained when performing single-
169 stage filtration, with catalyst retention in the retentate side approaching total rejection (99.4%
170 recovery) after the initial transient period when membrane compaction and equilibration with
171 the surrounding environment resulted in slowly improving filtration performance that
172 stabilized over a few hours. Despite the high catalyst recovery, limited flux through the
173 membrane resulted in a relatively low permeate volume, which in turn affected the overall
174 product recovery for a single stage (48.1%), since a large fraction of the product remained in
175 the retentate volume. It should be noted that the product transport through the membrane is
176 not selective, resulting in equal concentrations in permeate and retentate. For this reason,
177 the product recovery is only dependent on the permeate-to-retentate volumetric ratio.
178 Therefore, to increase the overall permeate volume and in turn product recovery, a second
179 filtration stage was added to the process, where the retentate solution still containing a
180 relatively large amount of product was filtered through a second OSN unit. Given the smaller
181 input volume, the second filtration had a lower flow rate, which resulted in equilibrium flux
182 values lower than for the first stage, in line with the results of the flow rate screening for
183 filtration of TBADT solutions. For the second stage, catalyst retention exceeded 99%,
184 resulting in a combined catalyst recovery of 98.4% over the two stages paired with a
185 satisfactory product recovery exceeding 80%. The results of these experiments highlighted
186 the trade-off between the catalyst recovery and the product recovery for a membrane with
187 limited flux and high chemical resistance. Nevertheless, the two-stage filtration design

enabled overcoming the trade-off and delivered high catalyst recovery coupled with suitable product recovery.

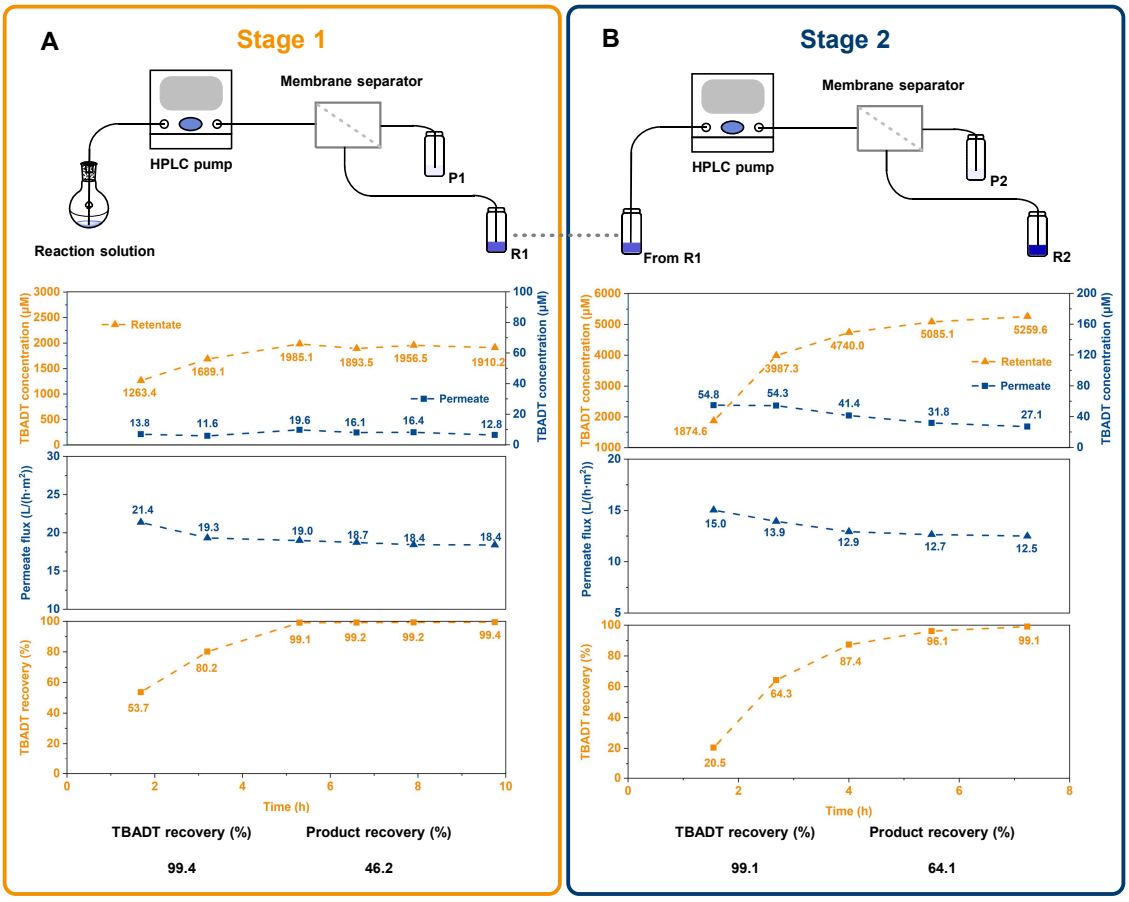

Figure 1. (A) Results of the nanofiltration experiment of the reacted mixture (Stage 1): concentration of TBADT in the retentate and permeate; permeate flux; catalyst and product recovery. (B) Results of the nanofiltration experiment of the retentate solution from stage 1 (Stage 2): concentration of TBADT in the retentate and permeate; permeate flux; catalyst and product recovery. (C) Summary of the overall recovery process for the two NF stages.

Given the results of the batch study, a continuous-flow hydroalkylation reaction with in-line catalyst recovery was designed (Scheme 1b). After equilibrating the system during the start-up phase, in-line catalyst recycling was initiated by feeding back the retentate from the second OSN stage to the mixture of dimethyl maleate and cyclohexane in acetonitrile. A first

run of 19 hours was performed, achieving total TONs of 2659. The product yield measured throughout the experiment was close to that of the optimized reaction performed with pristine TBADT and only decreased toward the end of the experiments. This is explained by a decrease in the catalyst concentration towards the end of the experiment, which was the consequence of the peristaltic pump used to deliver the substrate solution slowly deviating from its calibrated values and increasing the effective flow rate delivered to the holding tank. This resulted in extra dilution of the catalyst in the dimethyl maleate solution, leading to a decreased fraction yield.

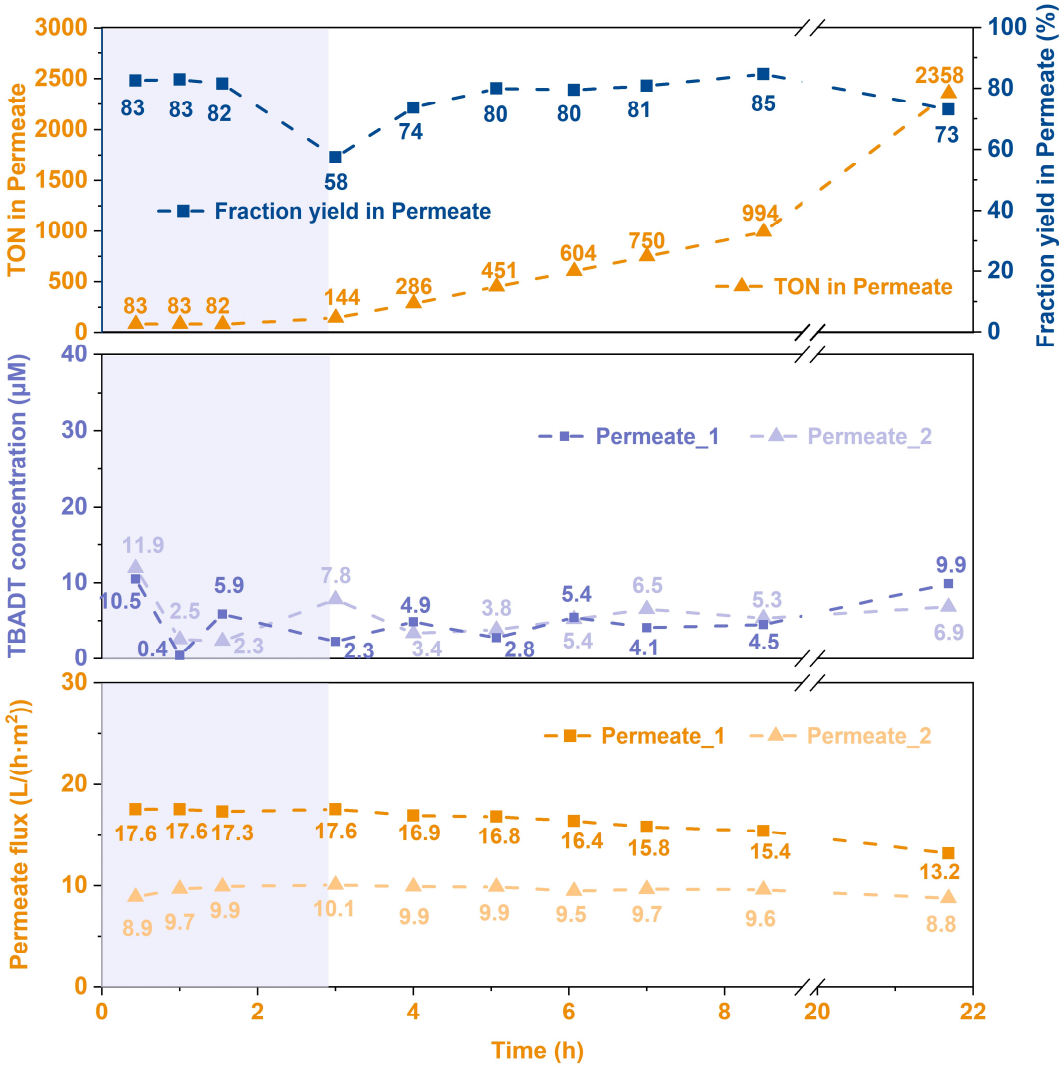

Figure 2. Results of the inline catalyst recovery experiment: turnover number and measured reaction yield; residual TBADT concentration in the permeate solution; permeate flux. The equilibration phase of the experiment is reported with a shaded background.

Given the promising results of the 19-hours run, a 3-day catalyst recycling experiment was performed (Figure 4). Throughout this period, the fraction yield of the model alkylation oscillated in a narrow range of 79 – 84%, and a total TON of 6738 (including additional 373 TONs remaining in the system) was achieved by the end of the 3-day catalyst recycling experiment. Notably, for this longer experimental run, some precipitation of TBADT on the membrane surface was detected during disassembly. The presence of fouling on the membrane surface explains the observed membrane flux decrease. Nevertheless, the deposited TBADT on the membrane surface could be easily washed away with pure acetonitrile. Therefore, to address the issue of catalyst deposition on the membrane surface, periodical (back)washing of the membrane with pure solvent could be implemented (e.g., 10 min wash with acetonitrile for every 8 hours of operation).

The in-line TBADT recovery proves the potential of OSN for catalyst recovery, thus helping bridge the gap between small-scale HAT transformation and their scaled-up counterparts. To further highlight the potential of this technique, a small scope for the model photocatalytic hydroalkylation was performed, reporting both the product yield for the reaction carried out with pristine TBADT and the product yield for the reaction performed with the in-line catalyst recovery configuration depicted in Scheme 1. Different electron-deficient alkenes, including esters and fumaronitrile were all good Michael acceptors, delivering good yields of the targeted products (**1** to **3**). Cyclopentane underwent the C–C bond forming reaction promptly, transforming unactivated alkyl substrate into targeted hydroalkylated compound (**4**). Esters (1,3-dioxolane and 1,4-dioxane) were used as H-donors for the radical addition on dimethyl maleate, which afforded the targeted products (**5**, **6**) in excellent yields. Promisingly, for all entries in the scope, the product yields are similar

for to those obtained without catalyst recycling, proving the generality of our inline catalyst recycling strategy.

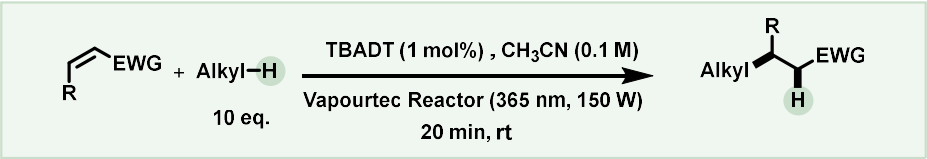

	1	2	3
No catalyst recycling:	87%[b] (84%)	91% (86%)	79% (71%)
With inline nanofiltration[b]:	85%	86%	64%
Turnover number:	2659 in 18.7 h	1592 in 12.1 h	1177 in 13 h

	4	5	6
No catalyst recycling:	73% (69%)	88%[c] (80%, H_A:H_B 2.2:1, H_B 1.5:1 d.r.)	96%[c] (86%, 1:1 d.r.)
With inline nanofiltration[b]:	65%	89%	94%
Turnover number:	1004 in 10.7 h	1201 in 14 h	2148 in 15.8 h

Figure 3. Scope of the photocatalytic C(sp^3)–H alkylation executed with inline TBADT recovery. [a] Reaction conditions for single run without catalyst recycling: alkene (0.1 M), H-donor (10 equiv), TBADT (1 mol%) in CH_3CN (5 mL). Irradiation source: λ = 365 nm (150 W), residence time: 5 min (see the supplementary information for additional details). Isolated yields are given in parentheses. [b] The yield was determined by ^{1}H-NMR using 1,2,4,5-tetramethylbenzene as external standard. [c] 1.2 mol% TBADT.

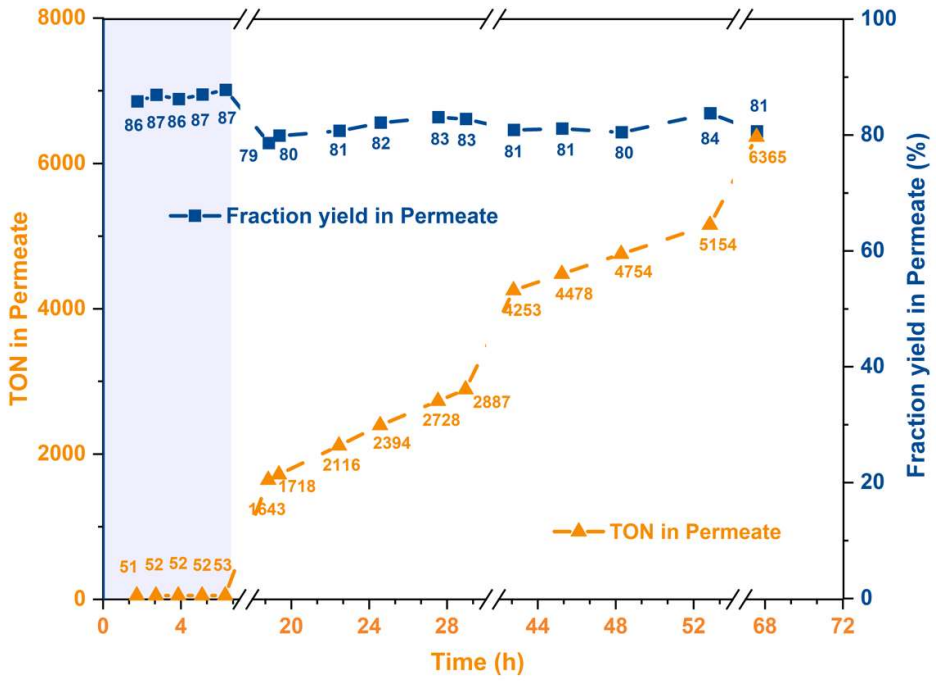

Figure 4. Fraction yield and TON in permeate of a 60-h run of C(sp^3)–H alkylation executed with inline TBADT recovery. The equilibration phase of the experiment is reported with a shaded background.

To conclude, this work presents in-line TBADT recovery as the answer to the concerns surrounding scale-up of TBADT-catalyzed photocatalytic HAT reactions, where catalyst consumption, cost, and removal are major concerns. A suitable OSN membrane was identified, and the operating conditions and experimental design were optimized to achieve suitable catalyst and product recovery. Notably, the product yield of reactions performed with in-line catalyst recovery are comparable to those carried out with pristine catalyst, proving that not only TBADT recovery is technically feasible, but it also does not compromise reaction performance. Considering the widespread interest in decatungstate-enabled HAT photocatalysis, we expect this inline catalyst recovery protocol will be particularly useful for process chemists to reduce the overall operational cost of the scaled-up process.

Method

General procedure for C(sp^3)-H alkylation with inline TBADT recovery. A 50 mL volumetric flask was charged with olefin (0.1 M, 5 mmol, 1 equiv.), H-donors (1 M, 50 mmol,

10 equiv.) and tetrabutylammonium decatungstate (TBADT) (1 mM, 50 μmol, 1 mol%). Next, CH_3CN was added to acquire a total volume of 50 mL. The prepared solution was transferred to the holding tank and delivered to a Vapourtec UV-150 Reactor (PFA tubing, 3.06 mL, 750 μm inner diameter) via HPLC pump. The outlet solution of photoreactor directly injected into the two-stage flow cells. Samples from permeate and retentate solutions were collected and analyzed until reaching the equilibrium of the membrane. Another solution with olefin and H-donors in acetonitrile was prepared, which was delivered to the holding tank by the peristaltic pump. Meanwhile, the retentate feed was put into the holding tank, mixing with the fresh starting material solution. The samples were collected from two permeate feeds and analyzed with ^1H NMR. After certain experimental time, a pure acetonitrile was used to push out the solution left inside the system. A total turnover number was calculated by combining solutions in permeate feeds and remaining in the system. A detailed description of the experimental setup and protocols is available in Section 3.2 of the Supplementary Information.

Acknowledgments

Z.W. acknowledges support from the China Scholarship Council (CSC, No. 201808440313). T.N. & D.P. acknowledge support from the European Commission via the Flow chemistry for Isotopic eXchange project (FLIX, grant agreement 862179) and from the Dutch Organization for Scientific Research (Nederlandse Organisatie voor Wetenschappelijk Onderzoek, NWO) via the Multi Modal Photochemistry project (grant agreement 18433).

Data availability

The authors declare that all relevant data supporting the findings of this study are available within the article and Supplementary Information files, and also are available from the corresponding author upon reasonable request.

Supplementary Information

Electronic supplementary information is available online at <URL>.

References

1. Capaldo L, Ravelli D, Fagnoni M. Direct Photocatalyzed Hydrogen Atom Transfer (HAT) for Aliphatic C–H Bonds Elaboration. *Chem Rev* **122**, 1875-1924 (2022).
2. Bonciolini S, Noël T, Capaldo L. Synthetic Applications of Photocatalyzed Halogen-radical mediated Hydrogen Atom Transfer for C−H Bond Functionalization. *Eur J Org Chem*, DOI: org/10.1002/ejoc.202200417 (2022).
3. Laudadio G, Deng Y, van der Wal K, Ravelli D, Nuño M, Fagnoni M, Guthrie D, Sun Y, Noël T. C(sp^3)–H functionalizations of light hydrocarbons using decatungstate photocatalysis in flow. *Science* **369**, 92-96 (2020).
4. Wen Z, Maheshwari A, Sambiagio C, Deng Y, Laudadio G, Van Aken K, Sun Y, Gemoets HPL, Noël T. Optimization of a Decatungstate-Catalyzed C(sp^3)–H Alkylation Using a Continuous Oscillatory Millistructured Photoreactor. *Org Process Res Dev* **24**, 2356-2361 (2020).
5. Fukuyama T, Nishikawa T, Yamada K, Ravelli D, Fagnoni M, Ryu I. Photocatalyzed Site-Selective C(sp^3)–H Functionalization of Alkylpyridines at Non-Benzylic Positions. *Org Lett* **19**, 6436-6439 (2017).
6. Murphy JJ, Bastida D, Paria S, Fagnoni M, Melchiorre P. Asymmetric catalytic formation of quaternary carbons by iminium ion trapping of radicals. *Nature* **532**, 218-222 (2016).
7. Protti S, Ravelli D, Fagnoni M, Albini A. Solar light-driven photocatalyzed alkylations. Chemistry on the window ledge. *Chem Commun*, 7351-7353 (2009).
8. Capaldo L, Bonciolini S, Pulcinella A, Nuno M, Noel T. Modular allylation of C(sp^3)−H bonds by combining decatungstate photocatalysis and HWE olefination in flow. *ChemRxiv*, DOI: 10.26434/chemrxiv-2021-5vdm7 (2021).
9. Perry IB, Brewer TF, Sarver PJ, Schultz DM, DiRocco DA, MacMillan DWC. Direct arylation of strong aliphatic C–H bonds. *Nature* **560**, 70-75 (2018).
10. Mazzarella D, Pulcinella A, Bovy L, Broersma R, Noël T. Rapid and Direct Photocatalytic C(sp^3)−H Acylation and Arylation in Flow. *Angew Chem Int Ed* **60**, 21277-21282 (2021).
11. Wan T, Wen Z, Laudadio G, Capaldo L, Lammers R, Rincón JA, García-Losada P, Mateos C, Frederick MO, Broersma R, Noël T. Accelerated and Scalable C(sp^3)–H Amination via Decatungstate Photocatalysis Using a Flow Photoreactor Equipped with High-Intensity LEDs. *ACS Cent Sci* **8**, 51-56 (2022).
12. Wan T, Capaldo L, Laudadio G, Nyuchev AV, Rincón JA, García-Losada P, Mateos C, Frederick MO, Nuño M, Noël T. Decatungstate-Mediated C(sp^3)–H Heteroarylation via Radical-Polar Crossover in Batch and Flow. *Angew Chem Int Ed* **60**, 17893-17897 (2021).

13. Bonassi F, Ravelli D, Protti S, Fagnoni M. Decatungstate Photocatalyzed Acylations and Alkylations in Flow via Hydrogen Atom Transfer. *Adv. Synth. Catal.* **357**, 3687-3695 (2015).
14. Ryu I, Tani A, Fukuyama T, Ravelli D, Montanaro S, Fagnoni M. Efficient C–H/C–N and C–H/C–CO–N Conversion via Decatungstate-Photoinduced Alkylation of Diisopropyl Azodicarboxylate. *Org Lett* **15**, 2554-2557 (2013).
15. Nodwell MB, Yang H, Čolović M, Yuan Z, Merkens H, Martin RE, Bénard F, Schaffer P, Britton R. 18F-Fluorination of Unactivated C–H Bonds in Branched Aliphatic Amino Acids: Direct Synthesis of Oncological Positron Emission Tomography Imaging Agents. *J Am Chem Soc* **139**, 3595-3598 (2017).
16. Halperin SD, Kwon D, Holmes M, Regalado EL, Campeau L-C, DiRocco DA, Britton R. Development of a Direct Photocatalytic C–H Fluorination for the Preparative Synthesis of Odanacatib. *Org Lett* **17**, 5200-5203 (2015).
17. Halperin SD, Fan H, Chang S, Martin RE, Britton R. A Convenient Photocatalytic Fluorination of Unactivated C-H Bonds. *Angew Chem Int Ed* **53**, 4690-4693 (2014).
18. Sarver PJ, Bacauanu V, Schultz DM, DiRocco DA, Lam Y-h, Sherer EC, MacMillan DWC. The merger of decatungstate and copper catalysis to enable aliphatic C(sp^3)–H trifluoromethylation. *Nat Chem* **12**, 459-467 (2020).
19. Sarver PJ, Bissonnette NB, MacMillan DWC. Decatungstate-Catalyzed C(sp^3)–H Sulfinylation: Rapid Access to Diverse Organosulfur Functionality. *J Am Chem Soc*, (2021).
20. Laudadio G, Govaerts S, Wang Y, Ravelli D, Koolman HF, Fagnoni M, Djuric SW, Noël T. Selective C(sp^3)−H Aerobic Oxidation Enabled by Decatungstate Photocatalysis in Flow. *Angew Chem Int Ed* **57**, 4078-4082 (2018).
21. Schultz DM, Lévesque F, DiRocco DA, Reibarkh M, Ji Y, Joyce LA, Dropinski JF, Sheng H, Sherry BD, Davies IW. Oxyfunctionalization of the Remote C−H Bonds of Aliphatic Amines by Decatungstate Photocatalysis. *Angew Chem Int Ed* **56**, 15274-15278 (2017).
22. Hartwig JF. Evolution of C–H Bond Functionalization from Methane to Methodology. *J Am Chem Soc* **138**, 2-24 (2016).
23. Yasuda N. *The art of process chemistry*. John Wiley & Sons (2010).
24. Noël T, Zysman-Colman E. The promise and pitfalls of photocatalysis for organic synthesis. *Chem Catal* **2**, 468-476 (2022).
25. Peeva L, Burgal JdS, Valtcheva I, Livingston AG. Continuous purification of active pharmaceutical ingredients using multistage organic solvent nanofiltration membrane cascade. *Chem Eng Sci* **116**, 183-194 (2014).

26. Lévesque F, Di Maso MJ, Narsimhan K, Wismer MK, Naber JR. Design of a Kilogram Scale, Plug Flow Photoreactor Enabled by High Power LEDs. *Org Process Res Dev* **24**, 2935-2940 (2020).
27. Corcoran EB, McMullen JP, Lévesque F, Wismer MK, Naber JR. Photon Equivalents as a Parameter for Scaling Photoredox Reactions in Flow: Translation of Photocatalytic C−N Cross-Coupling from Lab Scale to Multikilogram Scale. *Angew Chem Int Ed* ***59,*** 11964-11968 (2020).
28. Harper KC, Moschetta EG, Bordawekar SV, Wittenberger SJ. A Laser Driven Flow Chemistry Platform for Scaling Photochemical Reactions with Visible Light. *ACS Cent Sci* **5**, 109-115 (2019).
29. Beatty JW, Douglas JJ, Miller R, McAtee RC, Cole KP, Stephenson CRJ. Photochemical Perfluoroalkylation with Pyridine N-Oxides: Mechanistic Insights and Performance on a Kilogram Scale. *Chem* **1**, 456-472 (2016).
30. Dong Z, Wen Z, Zhao F, Kuhn S, Noël T. Scale-up of micro- and milli-reactors: An overview of strategies, design principles and applications. *Chem Eng Sci X* **10**, 100097 (2021).
31. Buglioni L, Raymenants F, Slattery A, Zondag SDA, Noël T. Technological Innovations in Photochemistry for Organic Synthesis: Flow Chemistry, High-Throughput Experimentation, Scale-up, and Photoelectrochemistry. *Chem Rev* **122**, 2752-2906 (2022).
32. Peeva L, Da Silva Burgal J, Heckenast Z, Brazy F, Cazenave F, Livingston A. Continuous Consecutive Reactions with Inter-Reaction Solvent Exchange by Membrane Separation. *Angew Chem Int Ed* **55**, 13576-13579 (2016).
33. Vural Gürsel I, Noël T, Wang Q, Hessel V. Separation/recycling methods for homogeneous transition metal catalysts in continuous flow. *Green Chem* **17**, 2012-2026 (2015).
34. O'Neal EJ, Lee CH, Brathwaite J, Jensen KF. Continuous Nanofiltration and Recycle of an Asymmetric Ketone Hydrogenation Catalyst. *ACS Catal* **5**, 2615-2622 (2015).
35. Marchetti P, Jimenez Solomon MF, Szekely G, Livingston AG. Molecular Separation with Organic Solvent Nanofiltration: A Critical Review. *Chem Rev* **114**, 10735-10806 (2014).
36. Guerra J, Cantillo D, Kappe CO. Visible-light photoredox catalysis using a macromolecular ruthenium complex: reactivity and recovery by size-exclusion nanofiltration in continuous flow. *Catal Sci Technol* **6**, 4695-4699 (2016).
37. Peeva L, da Silva Burgal J, Vartak S, Livingston AG. Experimental strategies for increasing the catalyst turnover number in a continuous Heck coupling reaction. *J Catal* **306**, 190-201 (2013).

404 38. O'Neal EJ, Jensen KF. Continuous Nanofiltration and Recycle of a Metathesis
405 Catalyst in a Microflow System. *ChemCatChem* **6**, 3004-3011 (2014).
406 39. Devery Iii JJ, Douglas JJ, Nguyen JD, Cole KP, Flowers Ii RA, Stephenson CRJ.
407 Ligand functionalization as a deactivation pathway in a fac-Ir(ppy)3-mediated radical
408 addition. *Chem Sci* **6**, 537-541 (2015).
409